Lattice effects in multiferroic $R\mathrm{Mn_2O_5}$ (R=Sm–Dy, Y)

Makoto Tachibana, Keita Akiyama, Hitoshi Kawaji, and Tooru Atake
Materials and Structures Laboratory, Tokyo Institute of Technology, 4259 Nagatsuta-cho, Midori-ku, Yokohama 226-8503, Japan
(Received 8 September 2005; revised manuscript received 25 October 2005; published 19 December 2005)

The evolution of antiferromagnetic and ferroelectric transitions for the series of multiferroic $R\mathrm{Mn_2O_5}$ (R=Sm, Eu, Gd, Tb, Dy, and Y) has been investigated by heat capacity measurements on single crystals. Both transition temperatures increase monotonically with the decreasing size of R, which are correlated with the systematic changes in the structural parameters determined from synchrotron x-ray powder diffraction. For R=Eu, Tb, Dy, and Y, an additional transition associated with the Mn moments appears at a lower temperature, with no apparent systematic behavior as a function of the size of R.

DOI: 10.1103/PhysRevB.72.224425 PACS number(s): 75.30.Et, 77.80.−e, 64.70.Rh, 65.40.Ba

Systems with mutual coupling of ferroelectricity and magnetism, usually referred to as magnetoelectrics or multiferroics, have been the subject of great interest in recent years. In addition to the interest from basic scientific point of view, these systems may find important applications in multifunctional devices. In particular, the discovery of highly reproducible electric polarization reversal by a magnetic field in $\mathrm{TbMn_2O_5}$ (Ref. 1) and an extremely large magnetodielectric effect in $\mathrm{DyMn_2O_5}$ (Ref. 2) provide exciting opportunities for magnetically controlled ferroelectric devices. The intricate interplay between ferroelectricity and magnetism in these compounds appears to arise from competing interactions of the Mn moments, with incommensurate (IC) magnetic ordering and lattice modulations due to strong magnetoelastic coupling.[3,4]

Compounds with the general formula $R\mathrm{Mn_2O_5}$ (R=rare earth or Bi) crystallize in the orthorhombic structure (space group *Pbam*), where $\mathrm{Mn^{4+}O_6}$ octahedra share edges to form infinite chains along the c axis, and these chains are linked by pairs of $\mathrm{Mn^{3+}O_5}$ pyramids in the ab planes. From the complex crystal structure, five different nearest-neighbor interactions of the Mn moments, as shown in the inset of Fig. 1, can be identified. Furthermore, the geometrical frustration of these interactions[3,4] results in the appearance of a number of phase transitions in the low temperature region. At T_N, which is below 45 K, the $\mathrm{Mn^{4+}/Mn^{3+}}$ moments order antiferromagnetically with an IC magnetic propagation vector $\boldsymbol{k}=(k_x,0,k_z)$, where $k_x\sim0.5$ and $0\leqslant k_z\leqslant0.5$. $\mathrm{BiMn_2O_5}$ seems to be an exception, where a magnetic transition to a (0.5, 0, 0.5) structure has been reported.[5] At several Kelvin below T_N, the system shows a ferroelectric transition with the polarization along the b axis, and $\boldsymbol{k}$ becomes commensurate at or slightly below this transition. It has been widely speculated[3,6] that the ferroelectricity arises from small structural displacements that would lift the magnetic degeneracy, a plausible scenario considering the frustrated magnetic interactions. Recent synchrotron x-ray studies[7] found some evidence of lattice modulation in the ferroelectric phase of $\mathrm{DyMn_2O_5}$, though the atomic displacements seem to be extremely small.[3,4] On cooling down still further, additional magnetic transition at ~25 K is reported for some compounds, where $\boldsymbol{k}$ again becomes IC. It is below this transition where strong dependence of the dielectric constant on magnetic field is observed in $\mathrm{DyMn_2O_5}$.[2] Finally, the magnetic ordering of the R^{3+} moments occurs below 10 K.

Throughout the sequence of successive phase transitions, the propagation vector k_z shows complex variation that is closely associated with the changes in ferroelectric behavior.[3,8,9] The value of k_z also shows strong variation with R,[5] indicating the important role of the crystal lattice on the magnetic structure. However, systematic understanding has been hampered by strong absorption of neutron for R=Sm, Eu, and Gd, as well as difficulty in growing single crystals for some members of the lanthanides. Nonetheless, systematic studies of the transitions as a function of R should provide important insights into the nature of the interplay between crystal structure, magnetic order, and ferroelectricity in this class of compounds. In this paper, we report the temperature phase diagram for the magnetic and ferroelectric transitions in R=Sm–Dy and Y, as determined by heat capac-

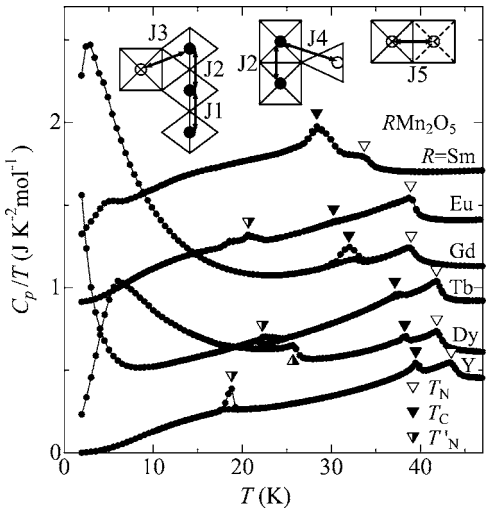

FIG. 1. Heat capacity divided by temperature for $R\mathrm{Mn_2O_5}$ (R=Sm, Eu, Gd, Tb, Dy, and Y). The data have been offset by 1.2, 0.9, 0.6, 0.3, 0, and 0 J K^{-2} mol^{-1}, respectively, for clarity. The open, closed, and half-closed triangles locate the transition temperatures of T_N, T_C, and T'_N, respectively. The inset shows structural components of $R\mathrm{Mn_2O_5}$ with the five types of nearest-neighbor magnetic interactions. Filled and empty circles represent $\mathrm{Mn^{4+}}$ and $\mathrm{Mn^{3+}}$, respectively.

ity measurements on single crystals. The phase diagram covers the R ions for which high-quality single crystals can be grown and includes the compounds where intriguing multiferroic behavior has been reported recently.[1,2] The phase diagram shows monotonic increase in both the magnetic and ferroelectric transition temperatures as the size of R decreases. Our structural study employing synchrotron x-ray powder diffraction shows that these trends are closely associated with the systematic changes in the crystal structure.

Single crystals of $R\mathrm{Mn_2O_5}$ (R=Sm, Eu, Gd, Tb, Dy, and Y) were grown in a Pt crucible using $\mathrm{B_2O_3}$, PbO, $\mathrm{PbO_2}$, and $\mathrm{PbF_2}$ as the flux.[10] It should be noted that single crystals of R=La, Pr, or Nd have not been produced by the same method, although polycrystalline samples of these compounds have been synthesized under high oxygen pressures[11] and small crystals of R=Nd have been produced by the chemical transport method.[12] To our knowledge, detailed physical properties of these compounds have not been reported. Likewise, the growth of high-quality single crystals by the flux method becomes difficult for R smaller than Er.[10,13] The powder x-ray diffraction patterns showed that the products are single phase. Heat capacity measurements were performed on a single crystal by the relaxation method, using a Quantum Design PPMS in both heating and cooling modes. The measurements were performed on several crystals for each compound to ensure reproducibility. Synchrotron x-ray powder diffraction measurements were performed at 300 K on the BL02B2 beamline at SPring-8, using a wavelength of 0.415 Å. Structural parameters were refined by the Rietveld method, using the program RIETAN-2000.[14] No significant deviation from full occupancy was observed, and all the variable atomic positions and isotropic thermal parameters were varied in the final refinement. Good agreement parameters were obtained in each case, with $R_{\mathrm{wp}}<5.5\%$, $R_{\mathrm{I}}<1.8\%$, $R_{\mathrm{F}}<0.95\%$, and $S<2.1$. In this paper, we focus on structural parameters that are directly relevant to the discussion on exchange interactions; tabulated results of all the refined parameters, as well as the temperature evolution of the structural properties, will be published elsewhere.[15]

The heat capacity divided by temperature, C_p/T, for $R\mathrm{Mn_2O_5}$ with R=Sm, Eu, Gd, Tb, Dy, and Y, is shown in Fig. 1. The data taken from measurements on both the heating and cooling directions are plotted, with the latter showing smaller C_p where thermal hysteresis is observed. For each compound, there are three or four anomalies in the C_p curve that can be attributed to magnetic or ferroelectric transition. The results for R=Tb and Dy are very similar to the recently published results.[2] The well-defined lambda anomaly observed in each compound at the highest temperatures marks the onset of antiferromagnetic (AF) transition at T_{N}. This transition is clearly second order, and the absence of significant rounding in the C_p anomaly testifies to the high quality of the crystals. For R=Sm, the larger anomaly immediately below T_{N} obscures the peak at T_{N}, but the peak is clearly identified when plotted as C_p vs T. At 5–10 K below T_{N}, each compound undergoes another transition that is identified as ferroelectric transition (with the Curie temperature T_{C}). The shape of the anomaly varies among the compounds, with larger anomalies observed in R=Sm and Gd. The presence of thermal hysteresis, which is identified for each R when plotted in large scales, indicates that this transition is first order. For R=Tb and Y, recent neutron scattering studies[3,16,17] have shown that T_{C} is several Kelvin higher than the temperature where the magnetic propagation vector $\boldsymbol{k}$ continuously locks in at (0.5, 0, 0.25). In agreement with the previous study,[2] there is no visible anomaly in C_p at the lock-in transition; this is perhaps due to an insignificant change in entropy associated with the continuous change of $\boldsymbol{k}$.

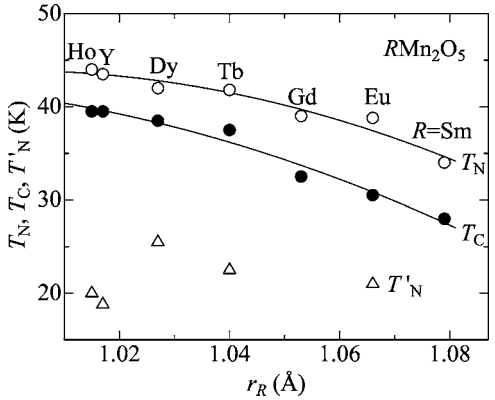

FIG. 2. Magnetic and ferroelectric phase diagram of $R\mathrm{Mn_2O_5}$ (R=Sm–Ho, Y) as a function of the ionic radius of R (r_R), where the peak position in heat capacity was taken as the transition temperature. The data for R=Ho are taken from Ref. 2. Ordering temperatures of the R^{3+} moments are not shown.

On further cooling, another transition is observed at $T'_{\mathrm{N}}=19-26$ K for R=Eu, Tb, Dy, and Y, but not for R=Sm and Gd. Moreover, thermal hysteresis can be identified for R=Eu, Tb, and Y. For R=Tb and Y, this transition has been identified as a reentrant magnetic transition where $\boldsymbol{k}$ once again becomes IC on cooling.[3,16,17] For isotopically substituted R=Eu, $\boldsymbol{k}$ remains unchanged at (0.5, 0, 0.33) across T'_{N}, and the transition involves an increase in the ordered moments of the $\mathrm{Mn^{4+}/Mn^{3+}}$ sublattice.[18] For R=Dy, more complex behavior has been reported.[4,7,9] The double peak observed for R=Eu was reproducible on several crystals, and similar feature was observed in a previous study employing dielectric constant measurements.[19] Extrinsic effects from sample inhomogeneity cannot be ruled out, however. The absence of the anomaly for R=Sm and Gd may be associated with the large anomaly observed at T_{C}, possibly implying that they have different sequence of $\boldsymbol{k}$ variations from other members of $R\mathrm{Mn_2O_5}$. On the other hand, the reentrant magnetic transition is also absent in R=Er,[20] but in this case the changes in k_z at other transitions seem to be similar to the cases of R=Y and Tb.[3,16,17] Neutron scattering measurements on isotopically substituted R=Sm and Gd are of great interest, as they should provide significant insights on the systematics of the k_z variation with R. For magnetic R (Sm, Gd, Tb, and Dy), another anomaly is observed below 10 K due to the ordering of the R^{3+} moments.

In Fig. 2, we show the phase diagram for $R\mathrm{Mn_2O_5}$ as a function of the ionic radius[21] of R (r_R) and temperature. For R=Ho, the C_p data from Ref. 2 are used to locate the transition temperatures. The figure clearly demonstrates that both

T_N and T_C monotonically increase with decreasing r_R, with a gradual decrease of the temperature interval between the two transitions. These concurrent systematic variations in T_N and T_C further support the magnetoelastically induced ferroelectricity in $R\mathrm{Mn_2O_5}$, and underscore the important lattice effects on the Mn spin interactions. With decreasing r_R, both T_N and T_C appear to approach a constant value, and this trend continues after R=Ho, where T_N=44 K and T_C=39.1 K for R=Er (Ref. 20) and T_N=44 K and T_C=36.4 K for R=Tm (Ref. 8) have been reported. The reason for the decrease in T_C for R=Tm is not clear, but it may be related to the difficulty in growing high-quality crystals for R smaller than Er.[10,13] Also, the present results are different from previous studies by Kohn and co-workers,[22] where some of the transitions appeared at lower temperatures and different variations as a function of r_R were shown in their phase diagram. The discrepancy is most likely due to the lower quality of the crystals employed in the earlier studies, as already pointed out in recent studies.[1,16] In contrast to the systematic behavior in T_N and T_C, T_N' shows no obvious correlation with r_R. Consequently, the role of f-d exchange interactions[7] cannot be ruled out for this transition, although we do not find clear relationship between T_N' and the R^{3+} moments.

As schematically shown in the inset of Fig. 1, the crystal structure of $R\mathrm{Mn_2O_5}$ consists of $\mathrm{Mn^{4+}O_6}$ octahedra and $\mathrm{Mn^{3+}O_5}$ pyramids, and various connectivity of these polyhedra lead to five different nearest-neighbor interactions. The $\mathrm{Mn^{4+}O_6}$ octahedra share common edges O2-O2 at the R layer (resulting in the exchange interaction labeled J1 in Fig. 1) and O3-O3 at the $\mathrm{Mn^{3+}}$ layer (J2) to form a chain along the c axis. Two $\mathrm{Mn^{3+}O_5}$ pyramids are connected to each other at the edge of their bases O1-O1 (J5), and these pyramids are connected to the octahedra through the apex oxygen O3 (J4) or base oxygen O4 (J3). For J1–J5, superexchange interactions involving Mn-O-Mn connectivity are operative. In addition, the Mn-Mn separation across the shared edges is short enough for both the octahedra (J1 and J2) and pyramids (J5) that there is dominant contribution from the direct exchange for these interactions.[3,4]

Figure 3 displays the variation of the lattice parameters a, b, and c and various Mn-O bond distances as a function of r_R. The present results show good overall agreement with the previous studies,[11,22] and the lattice parameters and the R-O distances (not shown) clearly scale with r_R. The change in lattice parameters is rather anisotropic, showing the largest variation along the a axis (2.2% between R=Y and Sm) and the smallest variation along the c axis (0.4% between R=Y and Sm). On the other hand, most of the Mn-O distances show only weak dependence on r_R, with the variation of the order of 0.02 Å. One exception is the $\mathrm{Mn^{3+}}$-O3 distance, where the results reveal a clear decrease of 0.05 Å between R=Sm and Y. It is worth pointing out that the identification of this deformable $\mathrm{Mn^{3+}}$-O3 bond is consistent with the proposed origin of the ferroelectricity,[3,4] which involves displacement of $\mathrm{Mn^{3+}}$ along the axis of the pyramids.

In Fig. 4, we show the variation of various bond angles Mn-O-Mn and bond distances Mn-Mn as a function of r_R. These parameters determine the strength of superexchange and direct-exchange interactions, respectively. Moreover, for J3 and J4, the associated bond angles are close to the ferro-

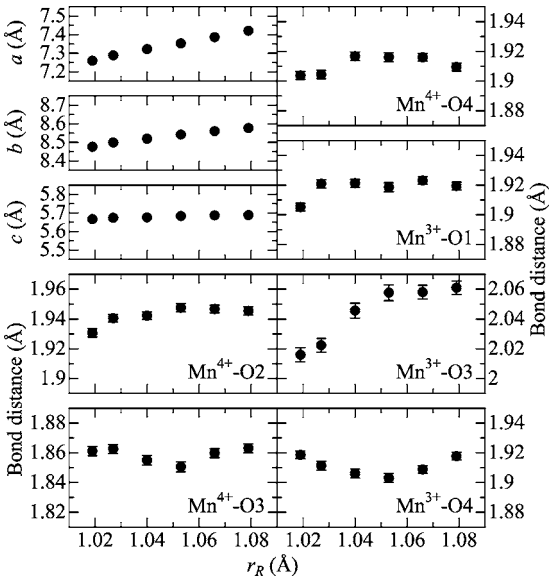

FIG. 3. Variation of the orthorhombic lattice parameters and Mn-O bond distances as a function of r_R.

magnetic (FM)/AF crossover.[3,4] Previous studies have established that the $\mathrm{Mn^{4+}}$-$\mathrm{Mn^{4+}}$ interaction at the $\mathrm{Mn^{3+}}$ layer is frustrated, since J3 and J4 always tend to align the $\mathrm{Mn^{4+}}$ parallel to each other, competing with the AF J2.[3,4] There is a significant increase of the $\mathrm{Mn^{4+}}$-$\mathrm{Mn^{4+}}$ distance at the $\mathrm{Mn^{3+}}$ layer with decreasing r_R, indicating that AF J2 is weakened with decreasing r_R. This should strengthen the tendency for a parallel alignment at the $\mathrm{Mn^{3+}}$ layer with decreasing r_R. On the other hand, the $\mathrm{Mn^{4+}}$-$\mathrm{Mn^{4+}}$ distance at the R layer shows the opposite trend, indicating that the AF J1 interaction is strengthened with decreasing r_R. For J1 and J2, weaker contributions from the superexchange interactions are FM,[3,4] but the small variations in the $\mathrm{Mn^{4+}}$-O-$\mathrm{Mn^{4+}}$ bond angles should

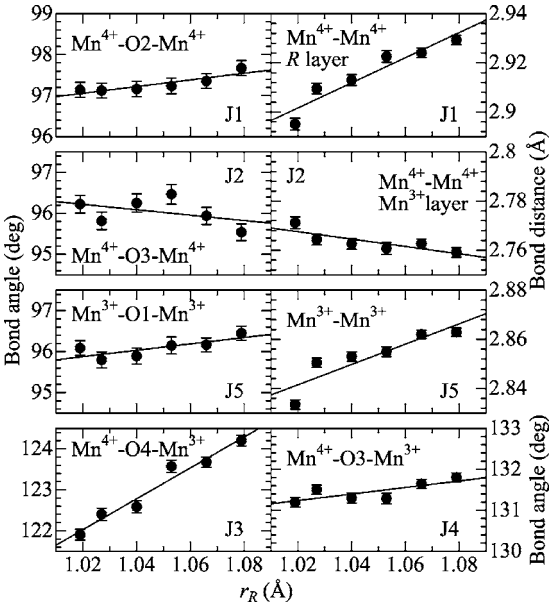

FIG. 4. Variation of the Mn-O-Mn bond angles and Mn-Mn bond distances as a function of r_R.

have marginal roles in determining the strength of overall interactions. Thus, the opposite trends in the strength of the AF interaction for the Mn^{3+} and R layers combine to produce manifold of stable superstructures along the c axis, as evidenced by the various k_z values reported for different R.[4,5]

The observed magnetic structure for the Mn^{4+}/Mn^{3+} layer,[3,4] which is essentially the same for various R, indicates that frustration is also operative in the ab plane. Especially, each Mn^{4+} moment has one nearest Mn^{3+} moment in the b direction that has a wrong sign, suggesting that $|J4| > |J3|$ and J4 is always AF.[3,4] Figure 4 shows that the bond angles associated with the J3 and J4 interactions decrease with decreasing r_R, possibly weakening the AF interaction for J4. However, this effect should be overshadowed by the very significant decrease in the Mn^{3+}-O3 distance, which would strengthen the AF interaction. The effects of bond-angle variation for J3 are not clear, but the stable magnetic structure for the Mn^{4+}/Mn^{3+} layer suggests that the character of J3 does not change significantly with r_R. For J5, the Mn^{3+}-Mn^{3+} distance smoothly decreases with decreasing r_R, strengthening the AF interaction.

The complex and frustrated nature of the interactions makes it difficult to disentangle the role of each interaction in changing T_N with r_R. However, the above discussion suggests that for J1, J5, and possibly J4, the AF interaction is strengthened with decreasing r_R. The AF J2 becomes weaker with decreasing r_R, but this interaction is competing with J3/J4 so that this tendency actually relieves the frustration and reinforces the magnetic ordering. Thus, the systematic changes in the structural parameters are in many respects consistent with the increase in T_N with decreasing r_R. Furthermore, the concomitant increase in T_C supports the notion that the ferroelectricity arises from magnetoelastically induced lattice modulation, which would relieve the spin frustration.[3,4]

In contrast to the systematic behavior observed for T_N and T_C, each member of RMn_2O_5 shows different multiferroic behavior in the low temperature region. Extremely large magnetodielectric effects are observed in R=Dy, whereas R=Tb and Ho show much smaller variation of the dielectric constant with magnetic field.[2] A complete reversal of polarization with the magnetic field is observed for R=Tb,[1] but others do not seem to show such a prominent effect.[2,7] These variations are apparently due to the additional roles played by the R^{3+} moments, the understanding of which will be the subject of future studies.

We thank Y. Kuroiwa for valuable discussions and assistance at SPring-8. The experiment at SPring-8 was performed with the approval of the Japan Synchrotron Radiation Research Institute (JASRI) No. 2005A0735. M.T. has been supported by JSPS.

[1] N. Hur, S. Park, P. A. Sharma, J. S. Ahn, S. Guha, and S.-W. Cheong, Nature (London) **429**, 392 (2004).
[2] N. Hur, S. Park, P. A. Sharma, S. Guha, and S.-W. Cheong, Phys. Rev. Lett. **93**, 107207 (2004).
[3] L. C. Chapon, G. R. Blake, M. J. Gutmann, S. Park, N. Hur, P. G. Radaelli, and S.-W. Cheong, Phys. Rev. Lett. **93**, 177402 (2004).
[4] G. R. Blake, L. C. Chapon, P. G. Radaelli, S. Park, N. Hur, S.-W. Cheong, and J. Rodriguez-Carvajal, Phys. Rev. B **71**, 214402 (2005).
[5] A. Muñoz, J. A. Alonso, M. T. Casais, M. J. Martinez-Lope, J. L. Martinez, and M. T. Fernandez-Diaz, Phys. Rev. B **65**, 144423 (2002).
[6] I. Kagomiya, S. Matsumoto, K. Kohn, Y. Fukuda, T. Shoubu, H. Kimura, Y. Noda, and N. Ikeda, Ferroelectrics **286**, 167 (2003).
[7] D. Higashiyama, S. Miyasaka, N. Kida, T. Arima, and Y. Tokura, Phys. Rev. B **70**, 174405 (2004).
[8] S. Kobayashi, H. Kimura, Y. Noda, and K. Kohn, J. Phys. Soc. Jpn. **74**, 458 (2005).
[9] W. Ratcliff II, V. Kiryukhin, M. Kenzelmann, S.-H. Lee, R. Erwin, J. Schefer, N. Hur, S. Park, and S.-W. Cheong, Phys. Rev. B **72**, 060407(R) (2005).
[10] B. M. Wanklyn, J. Mater. Sci. **7**, 813 (1972).
[11] J. A. Alonso, M. T. Casais, M. J. Martínez-Lope, J. L. Martínez, and M. T. Fernández-Diaz, J. Phys.: Condens. Matter **9**, 8515 (1997).
[12] P. Euzen, P. Leone, C. Gueho, and P. Palvadeau, Acta Crystallogr., Sect. C: Cryst. Struct. Commun. **49**, 1875 (1993).
[13] Y. Koyata, H. Nakamura, N. Iwata, A. Inomata, and K. Kohn, J. Phys. Soc. Jpn. **65**, 1383 (1996).
[14] F. Izumi and T. Ikeda, Mater. Sci. Forum **321–324**, 198 (2000).
[15] K. Akiyama *et al.* (unpublished).
[16] S. Kobayashi, T. Osawa, H. Kimura, Y. Noda, N. Kasahara, S. Mitsuda, and K. Kohn, J. Phys. Soc. Jpn. **73**, 3439 (2004).
[17] S. Kobayashi, T. Osawa, H. Kimura, Y. Noda, I. Kagomiya, and K. Kohn, J. Phys. Soc. Jpn. **73**, 1593 (2004).
[18] V. Polyakov, V. Plakhty, M. Bonnet, P. Burlet, L.-P. Regnault, S. Gavrilov, I. Zobkalo, and O. Smirnov, Physica B **297**, 208 (2001).
[19] E. I. Golovenchits, N. V. Morozov, V. A. Sanina, and L. M. Sapozhnikova, Sov. Phys. Solid State **34**, 56 (1992).
[20] S. Kobayashi, T. Osawa, H. Kimura, Y. Noda, I. Kagomiya, and K. Kohn, J. Phys. Soc. Jpn. **73**, 1031 (2004).
[21] R. D. Shannon, Acta Crystallogr., Sect. A: Cryst. Phys., Diffr., Theor. Gen. Crystallogr. **A32**, 751 (1976).
[22] I. Kagomiya, K. Kohn, and T. Uchiyama, Ferroelectrics **280**, 131 (2002), and references therein.